Am J Transl Res 2026;18(7):5547-5559
www.ajtr.org /ISSN:1943-8141/AJTR0172012

Original Article

Clinical significance of SNRPD1 expression in predicting post-transplant recurrence of hepatocellular carcinoma

Zhihong Wei[1,2*], Xuanhua Lin[1*], Jianwei Chen[1,2], Weidong Zhu[1], Jianyong Liu[1,2], Lizhi Lv[1,2], Fang Yang[1,2]

[1]Department of Hepatobiliary Surgery, Fuzong Clinical Medical College of Fujian Medical University, Fuzhou 350025, Fujian, China; [2]Department of Hepatobiliary Surgery, 900th Hospital of PLA Joint Logistic Support Force, Fuzhou 350025, Fujian, China. [*]Equal contributors.

Received February 10, 2026; Accepted May 15, 2026; Epub July 15, 2026; Published July 30, 2026

Abstract: Objective: To analyze SNRPD1 expression in hepatocellular carcinoma (HCC) and investigate its impact on post-liver transplantation recurrence and prognosis. Methods: Differentially expressed genes were identified from the TCGA-LIHC cohort using R-based bioinformatics tools. Kaplan-Meier survival analysis, ROC curves, nomograms, and Cox regression models assessed the diagnostic and prognostic value of SNRPD1 in HCC. Immunohistochemistry was performed to detect SNRPD1 protein expression in 102 paired HCC and adjacent non-tumor tissues, with correlation analysis of clinicopathological parameters and follow-up data. Results: SNRPD1 expression was significantly higher in HCC than in adjacent tissues (89.2% vs. 15.7%, $P < 0.001$) and positively correlated with microvascular invasion (MVI) and microvascular density (MVD) ($P < 0.05$; $r = 0.26$). Multivariate Cox regression confirmed high SNRPD1 expression as an independent risk factor for poor overall survival (hazard ratio (HR) = 0.679, $P < 0.001$) and progression-free survival (HR = 2.08, $P = 0.025$) in transplant recipients. The diagnostic AUC was 0.86. High SNRPD1 expression was associated with significantly shorter median overall survival (OS, 45 vs. 88 months) and progression-free survival (PFS, 46 vs. 75 months) (both $P < 0.01$). Conclusion: SNRPD1 is highly expressed in HCC and correlates with MVI and MVD. High SNRPD1 expression independently predicts poorer post-transplant OS and PFS, suggesting it as a promising prognostic biomarker and therapeutic target.

Keywords: SNRPD1, hepatocellular carcinoma, liver transplantation prognosis, microvascular invasion

Introduction

Hepatocellular carcinoma (HCC) represents a major global health challenge, with approximately 866,000 new cases and a third-highest mortality rate reported in 2022. China bears a substantial burden of HCC, with an incidence of 15.2 per 100,000 and a mortality rate of 12.6 per 100,000, accounting for nearly 50% of global cases [1, 2].

HCC is highly aggressive and prone to early metastasis. Approximately 70% of HCC patients exhibit no typical clinical symptoms in the early stages, resulting in most diagnoses occurring at intermediate to advanced stages, where the objective response rate to conventional therapies is less than 25% [3]. Although treatment strategies for HCC have increasingly adopted a multidisciplinary and multimodal approach, the overall 5-year survival rate remains poor at only 13.8% [4]. Even among the most effective curative options, such as liver transplantation, patients face a substantial risk of postoperative recurrence. Data indicate that the 5-year recurrence rate after HCC liver transplantation ranges from 20.0% to 57.8%, with a median survival of only 10.6-12.2 months after recurrence [5]. Therefore, further elucidation of the pathogenesis of HCC and the identification of novel tumor biomarkers and therapeutic targets are critical for improving overall prognosis and selecting suitable transplant candidates to reduce recurrence risk.

Studies have demonstrated that significant pre-mRNA splicing dysregulation occurs in the early stages of HCC, and this abnormality plays a critical role in tumorigenesis [6]. Pre-mRNA splicing is carried out by the spliceosome, a dynamic macromolecular ribonucleoprotein complex composed of five small nuclear ribonucleoproteins (snRNPs, each containing snRNA and associated proteins) along with multiple

https://doi.org/10.62347/WJUN3883

auxiliary proteins [7]. Among these, the SNRPD1 gene, located at 18q11.2 and containing a Sm core domain, plays a key role in snRNP complex assembly and exhibits oncogenic characteristics in cell cycle regulation [8]. Previous studies have shown that SNRPD1 is highly expressed in various cancers, including breast cancer and neuroblastoma, and is closely associated with tumor invasiveness [9, 10]. However, the role of SNRPD1 in HCC remains poorly understood, and its impact on post-liver transplantation recurrence and metastasis has not yet been reported.

To investigate the potential role of SNRPD1 in post-transplant HCC recurrence, we systematically analyzed its expression and correlations with clinicopathological parameters, and its impact on survival. Thereby establishing a theoretical basis for SNRPD1 as a prognostic predictor and therapeutic target.

Materials and methods

Bioinformatics analysis

Data acquisition and processing: RNA sequencing data and corresponding clinicopathological information for hepatocellular carcinoma were obtained from the TCGA public database (TCGA-LIHC cohort; [https://portal.gdc.cancer.gov/] (https://portal.gdc.cancer.gov/)), including a total of 373 samples. Raw expression data were normalized from fragments per kilobase per million reads (FPKM) to transcripts per million (TPM). All sample collection and data usage complied with the ethical guidelines of the National Institutes of Health (NIH).

Differential expression analysis: Samples were divided into high- and low-expression groups based on the median SNRPD1 expression level. Differentially expressed genes (DEGs) were identified using the LIMMA package (v1.26.0), with the criteria set as |log2 fold change (FC)| > 1 and adjusted *p*-value < 0.05. Volcano plots and heatmaps were generated using the ggplot2 package (v3.3.3).

Functional enrichment analysis: Gene Ontology (GO) term and Kyoto Encyclopedia of Genes and Genomes (KEGG) pathway enrichment analyses were performed for the DEGs using the ClusterProfiler package (v3.18.0). The top 15 significantly enriched terms and pathways were visualized ($P < 0.05$).

Immune cell infiltration analysis: The xCell algorithm implemented in the GSVA package (v1.34.0) was used to estimate the infiltration levels of 64 immune cell types. Spearman correlation analysis was conducted to evaluate the associations between SNRPD1 expression and immune cell infiltration as well as immune-related marker expression.

Evaluation of prognostic and diagnostic value: The TCGA-LIHC cohort was integrated with publicly available HCC survival datasets. Kaplan-Meier survival analysis and univariate and multivariate Cox proportional hazards regression analyses were performed using the “survival” (v3.2-10) and “survminer” (v0.4.9) packages. Diagnostic performance was assessed using the pROC package (v1.17.0.1) and time-dependent ROC analyses. ROC curves, nomograms, and calibration curves were constructed using ggplot2.

Experimental methods and clinical validation

Patient characteristics: We retrospectively collected clinical data from HCC patients who underwent liver transplantation at our hospital between January 2015 and December 2019. Inclusion criteria were: (1) meeting the Hangzhou criteria (maximum tumor diameter < 8 cm, or > 8 cm with preoperative alpha fetoprotein (AFP) < 400 ng/mL, moderate/high histological differentiation, no major vascular invasion or distant metastasis) [11]; (2) postoperative pathological confirmation of HCC; (3) no history of other primary malignancies; (4) complete baseline, pathological, and follow-up data. Exclusion criteria were: (1) extensive tumor necrosis or markedly reduced cellular density on postoperative pathology; (2) perioperative death within 30 days; (3) history of two or more liver transplantations. A total of 102 patients were included, followed up until February 28, 2025, or death, with a median follow-up of 64.5 months (range, 13-116 months). During follow-up, tumor recurrence occurred in 54 patients (52.9%) and 65 patients (63.7%) died. The study was approved by 900 Hospital of The Joint Logistics Team ethics committee.

Primary observational indicators: Baseline characteristics, including sex, age, tumor size and number, preoperative treatment history, and postoperative pathological indicators such as Edmondson grade, liver capsule invasion, microvascular invasion (MVI), satellite lesions,

and vascular tumor thrombi, were extracted from the hospital electronic medical record system. Postoperative HCC tissues and paired adjacent non-tumor paraffin-embedded specimens were collected for subsequent analyses.

Main reagents: Rabbit anti-human CD31 (#ab28364) and SNRPD1 (#ab272632) monoclonal antibodies, and HRP-labeled goat anti-rabbit IgG secondary antibodies (#ab205718), were purchased from Abcam, Cambridge, UK. Immunohistochemistry SP kits and DAB chromogenic kits were obtained from Chengdu Zhengneng Biotechnology Co., Ltd. Other routine reagents were provided by the hospital's basic medical laboratory.

Experimental methods: Continuous sections were prepared from paraffin-embedded HCC and adjacent non-tumor tissues. After deparaffinization and graded hydration, antigen retrieval was performed using citrate buffer (pH 6.0) with heat treatment. Endogenous peroxidase activity was blocked by incubation with 3% hydrogen peroxide at room temperature, and nonspecific binding sites were blocked with normal goat serum. Sections were incubated overnight at 4°C with primary antibodies against CD31 or SNRPD1. After thorough washing with PBS, secondary antibodies were applied and incubated at room temperature for 30-60 minutes, followed by DAB chromogenic development. Cell nuclei were counterstained with hematoxylin, and slides were dehydrated, cleared, and mounted with neutral resin. All experimental procedures were strictly controlled to ensure reliability and reproducibility.

Interpretation of results: All slides were independently evaluated in a double-blind manner by two experienced pathologists; disagreements were resolved by a third senior pathologist. Since this study is a retrospective study, only the final consensus value of the early cases was recorded in the database. SNRPD1 expression was scored by multiplying staining intensity (0-3) by the percentage of positive cells (0-4); a total score > 4 was defined as high expression, and ≤ 4 as low expression. Microvascular density (MVD) was assessed using CD31 as a marker following the Weidner counting method: the most vascularized area was identified under low magnification, and five random high-power fields were counted to calculate the mean MVD for each specimen. Patients were categorized into high or low MVD groups based on the mean value.

Statistical analysis: Data analysis was performed using IBM SPSS Statistics 27.0. Categorical variables were compared using the chi-square (χ^2) test, and Fisher's exact test was applied when expected frequencies were < 5. Spearman rank correlation analysis was used to assess the relationship between SNRPD1 expression and MVD. Survival curves for overall survival (OS) and progression-free survival (PFS) were generated using the Kaplan-Meier method, and differences between groups were compared with the Log-Rank test. Univariate and multivariate Cox proportional hazards regression models were employed to identify prognostic risk factors and determine independent predictors of outcome. For multivariate Cox regression, variable selection followed a two-step strategy: (1) variables with $P < 0.05$ in univariate analysis were included; (2) MVI, a clinically established prognostic factor ($P = 0.084$ in univariate analysis), was force-entered into the PFS model based on clinical importance. Collinearity was assessed using variance inflation factor (VIF) and tolerance; all VIF values were < 3 and tolerance > 0.1, indicating no significant collinearity. A P value < 0.05 was considered statistically significant.

Results

Differential expression of SNRPD1 in HCC

Analysis of the TCGA-LIHC dataset demonstrated that SNRPD1 expression was significantly higher in HCC tissues compared with adjacent non-tumorous tissues ($P < 0.05$; **Figure 1A**). Based on the median SNRPD1 expression, samples were divided into high- and low-expression groups, yielding 510 DEGs, of which 256 were upregulated and 254 were downregulated (**Figure 1B**). Hierarchical clustering heatmaps illustrated the co-expression patterns of the top 100 core DEGs (**Figure 1C**).

Functional enrichment analysis of SNRPD1-related DEGs

GO enrichment analysis revealed that the DEGs associated with SNRPD1 were significantly enriched in biological processes (BP) related to the cell cycle, including chromosome segrega-

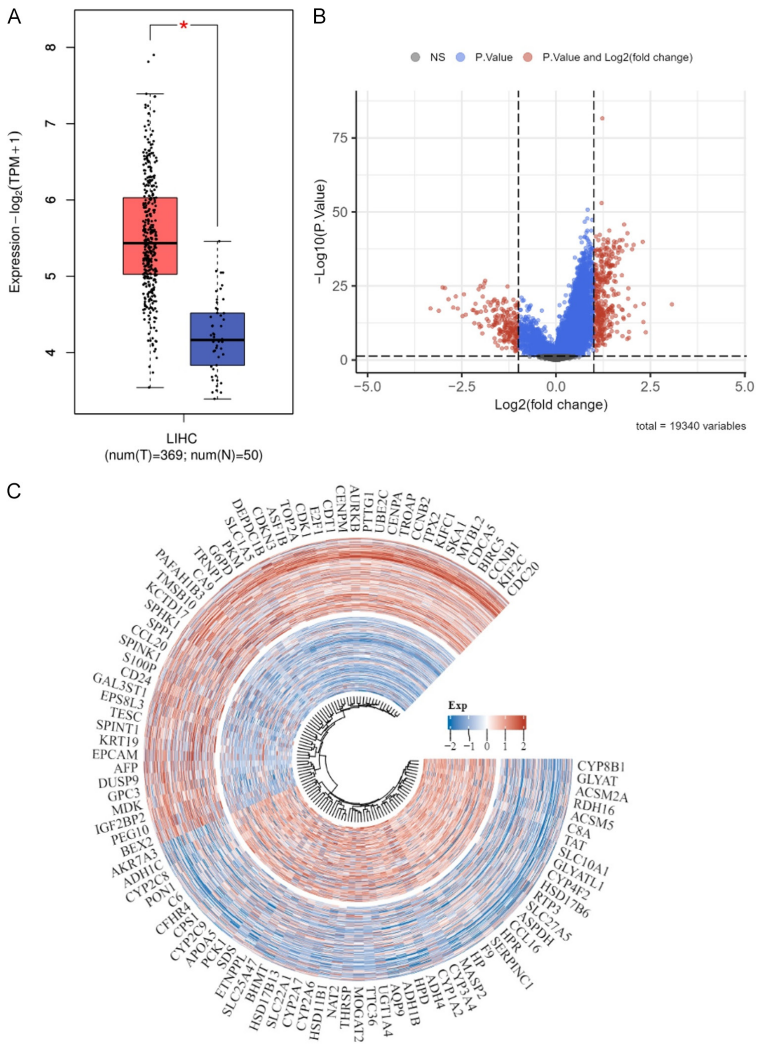

Figure 1. The expression of SNRPD1 is significantly upregulated in HCC. (A) In the TCGA-LIHC dataset, the expression level of SNRPD1 in HCC is significantly higher than that in the adjacent tissues; (B) The volcano plot and (C) the heatmap show the difference in mRNA expression levels between the high/low expression groups of SNRPD1 in HCC patients in the TCGA-LIHC dataset.

tion (40 genes), nuclear division (38 genes), and DNA replication (32 genes). In terms of molecular function (MF), DEGs were primarily enriched in ATPase activity (25 genes) and microtubule binding (22 genes). Regarding cellular components (CC), DEGs were enriched in condensed chromosomes (45 genes) and the spindle apparatus (38 genes) (**Figure 2**). KEGG pathway analysis showed significant enrichment in viral carcinogenesis (20 genes, -log10[P] = 15), the p53 signaling pathway (18 genes, -log10[P] = 12), and the IL-17 signaling pathway (15 genes, -log10[P] = 10), among others (**Figure 2**).

Correlation between SNRPD1 expression and immune cell infiltration

xCell analysis combined with Spearman correlation revealed that SNRPD1 expression was positively correlated with dendritic cells ($r = 0.222$, $P < 0.001$), B cells ($r = 0.345$, $P < 0.001$), $CD4^+$ memory T cells ($r = 0.189$, $P < 0.01$), naïve $CD4^+$ T cells ($r = 0.114$, $P < 0.05$), and $CD8^+$ T cells ($r = 0.086$, $P < 0.1$), while showing a negative correlation with $CD4^+$ central memory T cells ($r = -0.103$, $P < 0.05$) (**Figure 3**).

Prognostic and diagnostic potential of SNRPD1 in HCC

The clinical and pathological data of patients included in this study is shown in **Table 1**. Kaplan-Meier survival analysis demonstrated that patients with high SNRPD1 expression had a significantly shorter median overall survival (3.3 years) compared to those with low expression (5.8 years), with a log-rank $P = 0.000798$. The high-expression group exhibited a 1.822-fold higher risk of death than the low-expression group (95% CI: 1.283-2.588) (**Figure 4C**). Receiver operating characteristic (ROC) curve analysis indicated AUC values of 0.701, 0.631, and 0.643 for 1-, 3-, and 5-year survival, respectively, suggesting stronger predictive power for short-term prognosis (**Figure 4C**). Univariate Cox regression analysis identified SNRPD1 expression as a potential prognostic factor ($P = 3.23 \times 10^{-5}$, HR = 0.652, 95% CI: 0.345-0.959) (**Figure 4A**). Multivariate Cox regression confirmed SNRPD1 as an independent prognostic factor ($P = 0.00258$, HR = 0.679, 95% CI: 0.237-1.12) (**Figure 4B**). A nomogram incorporating SNRPD1 expression and pathological T stage was constructed, yielding a C-index of 0.675 (95% CI: 0.611-0.74). Calibration curves demonstrated good agree-

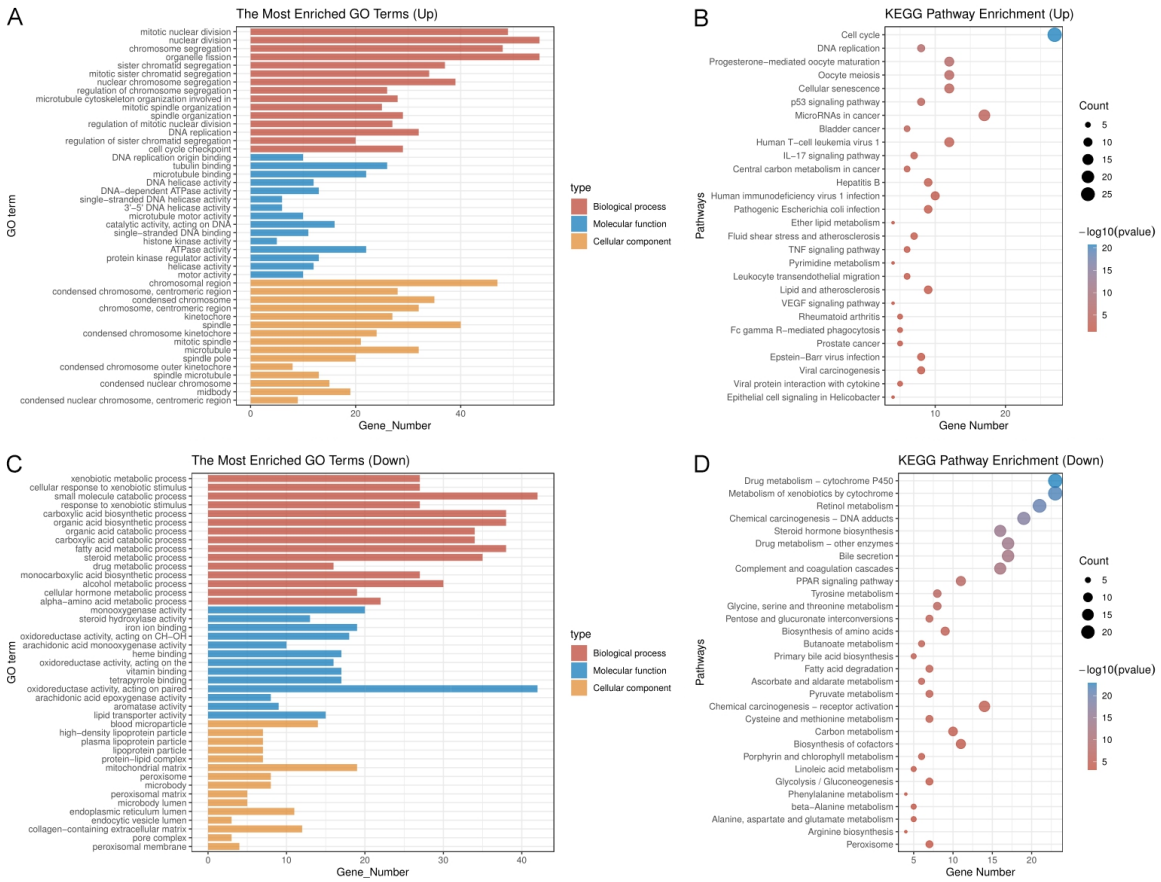

Figure 2. Functional enrichment analysis of DEGs based on the expression level of SNRPD1 in HCC. A. The GO enrichment results for up-regulated DEGs; B. The GO enrichment results for down-regulated DEGs; C. The KEGG pathway enrichment results for up-regulated DEGs; D. The KEGG pathway enrichment results for down-regulated DEGs.

ment between predicted and observed survival outcomes (**Figure 4D**, **4E**).

Immunohistochemical analysis of SNRPD1 expression in HCC and adjacent tissues

Immunohistochemical staining demonstrated that SNRPD1 protein was predominantly localized in the nucleus, exhibiting dark red granular deposition (**Figure 5A-D**). In HCC tissues, the high-expression rate of SNRPD1 was 89.2% (91/102), significantly higher than that in adjacent non-tumorous tissues, which was 15.7% (16/102). The difference was statistically significant ($P < 0.001$; **Table 2**).

Correlation between SNRPD1 expression and clinicopathological features

Correlation analysis revealed that SNRPD1 expression was significantly associated with MVI ($P < 0.05$). No significant associations were observed between SNRPD1 expression and other clinicopathological parameters, including sex, age, tumor number, maximum tumor diameter, AFP level, histological differentiation, liver capsule invasion, vascular tumor thrombus, or satellite lesions (all $P > 0.05$; **Table 3**).

Correlation between SNRPD1 expression and MVD

Among the 102 HCC tissue samples, 91 cases were SNRPD1-positive, including 68 cases with high MVD; 11 cases were SNRPD1-negative, including 34 cases with low MVD. A total of 65 cases were double-positive and 8 cases were double-negative. Spearman correlation analysis demonstrated a significant positive correlation between SNRPD1 expression and MVD ($r = 0.26$, $P < 0.05$; **Table 4**).

Association between SNRPD1 expression and post-transplant prognosis in HCC

SNRPD1 expression and PFS: Kaplan-Meier analysis demonstrated that the median PFS

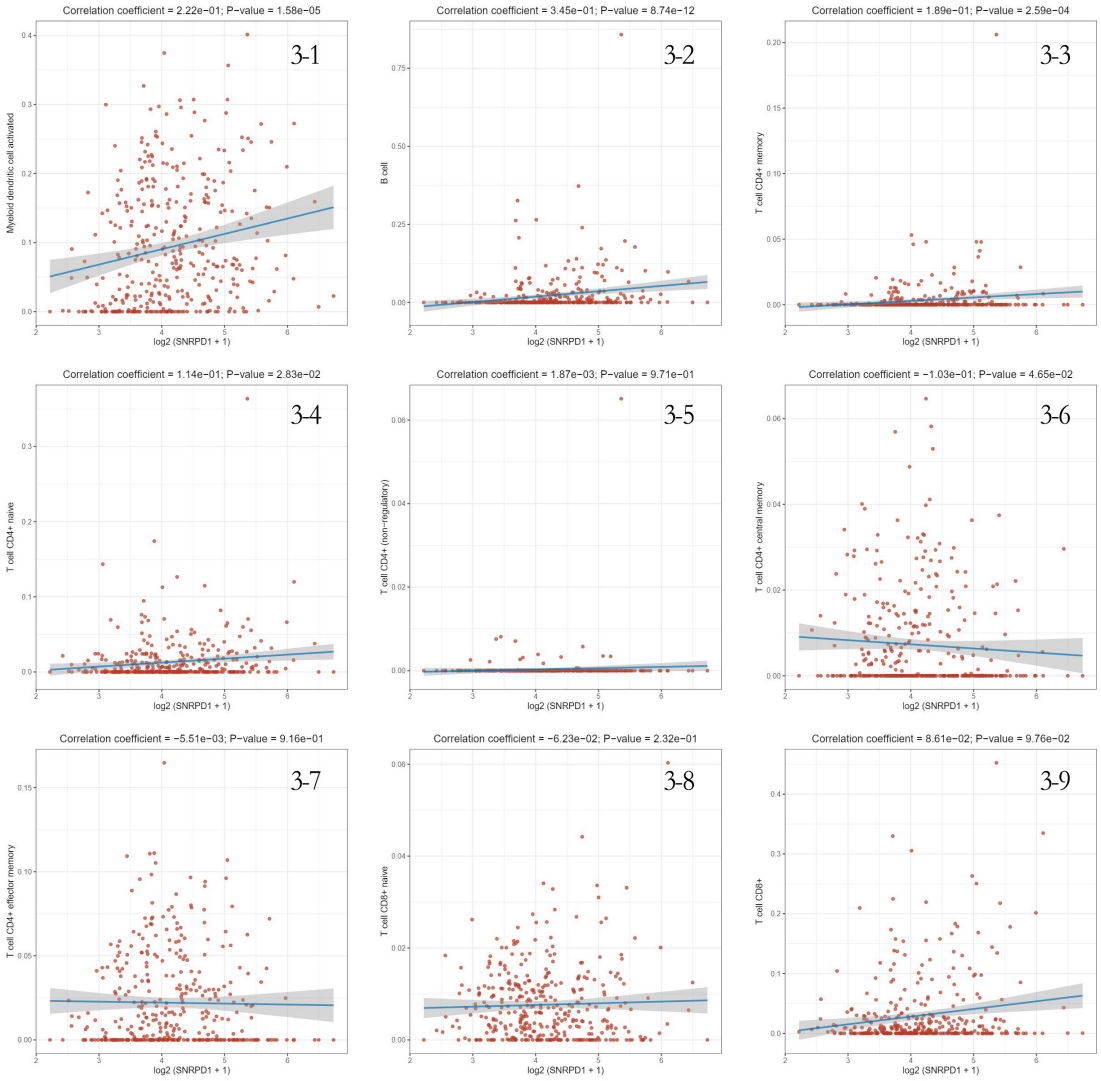

Figure 3. Correlation between SNRPD1 expression and immune cell infiltration.

Table 1. Clinical and pathological data of patients

Clinical data	Case	Clinical data	Case
Gender		Differential type	
Man	90	I-II	87
Woman	12	III-IV	15
Age (years)		Invasion of the liver capsule	
≤ 55	61	No	50
> 55	41	Yes	52
Number of tumors		MVI	
Single	63	No	34
More	39	Yes	68
Maximum tumor diameter (cm)		Vascular tumor thrombus	
≤ 5	59	No	49
> 5	43	Yes	53
Preoperative AFP level (ng/ml)		Satellite cooker	
≤ 400	66	No	77
> 400	36	Yes	25

*MVI: Microvascular Invasion.

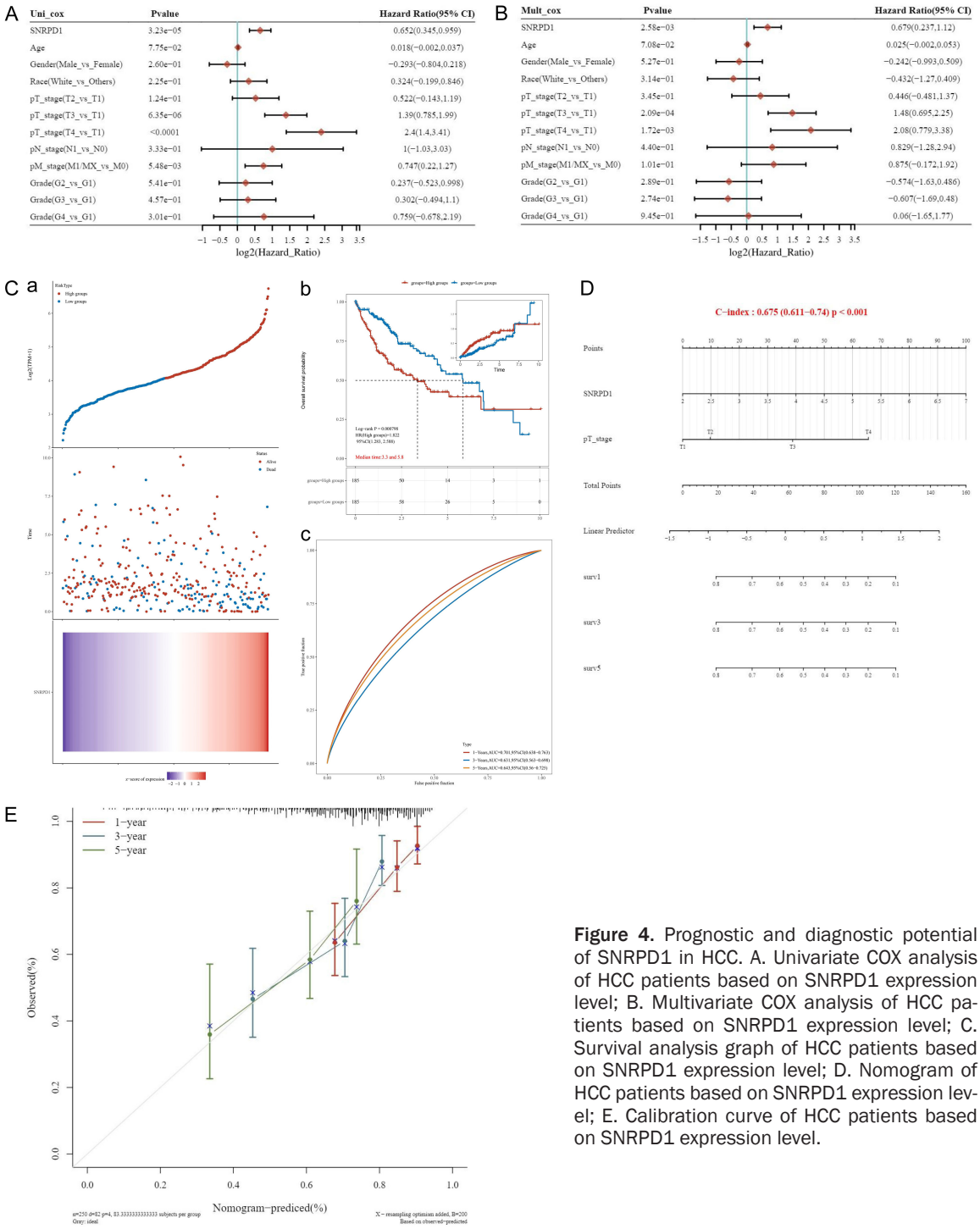

Figure 4. Prognostic and diagnostic potential of SNRPD1 in HCC. A. Univariate COX analysis of HCC patients based on SNRPD1 expression level; B. Multivariate COX analysis of HCC patients based on SNRPD1 expression level; C. Survival analysis graph of HCC patients based on SNRPD1 expression level; D. Nomogram of HCC patients based on SNRPD1 expression level; E. Calibration curve of HCC patients based on SNRPD1 expression level.

was 46 months in the high SNRPD1 expression group and 75 months in the low expression group. The difference was statistically significant (Log-rank P < 0.001; **Figure 6**), indicating a higher risk of postoperative recurrence in patients with high SNRPD1 expression.

SNRPD1 expression and OS: The median OS was 45 months in the high-expression group versus 88 months in the low-expression group, with a significant difference (Log-rank P < 0.001; **Figure 7**), suggesting that high SNRPD1 expression is associated with poorer post-transplant survival.

Prognostic factor analysis: Univariate Cox regression analysis showed that high SNRPD1 expression, liver capsule invasion, vascular

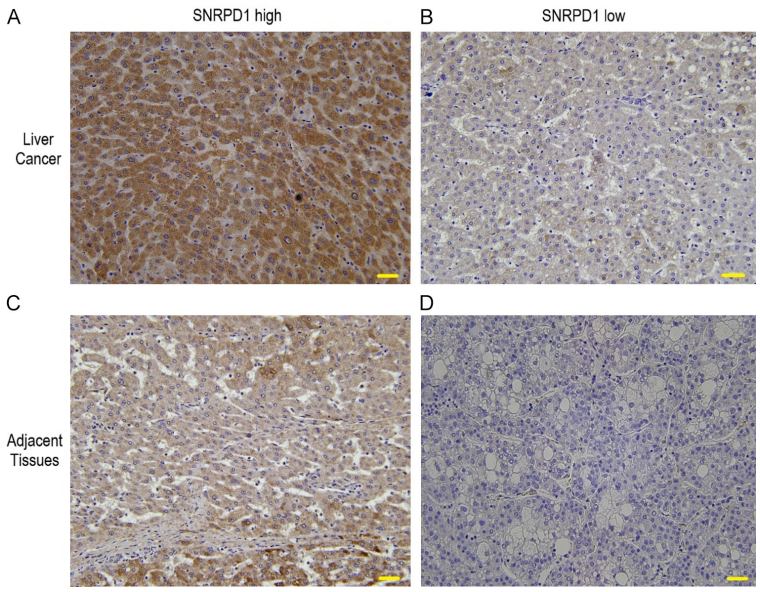

Figure 5. Immunohistochemical staining of SNRPD1 in HCC and adjacent tissues. A. High expression of SNRPD1 in liver cancer (20×); B. Low expression of SNRPD1 in liver cancer (20×); C. High expression of SNRPD1 in the surrounding area of the tumor (20×); D. Low expression of SNRPD1 in the surrounding area of the tumor (20×); Bar = 200 μm.

tumor thrombus, and satellite lesions were associated with PFS ($P < 0.05$). Although MVI showed only marginal significance in univariate analysis ($P = 0.084$), it was retained in the multivariate model due to its established clinical importance as a well-documented independent risk factor for HCC recurrence after liver transplantation and its role as a core component of the Hangzhou criteria used for patient selection in this study. Multivariate analysis revealed that after adjusting for confounders, MVI demonstrated independent prognostic value for PFS (HR = 2.10, 95% CI: 1.12-3.92, P = 0.020).

Multivariate analysis confirmed that high SNRPD1 expression (HR = 2.08, 95% CI: 1.09-3.95, P = 0.025), liver capsule invasion (HR = 3.25, 95% CI: 1.51-6.98, P = 0.003), and vascular tumor thrombus (HR = 2.34, 95% CI: 1.19-4.64, P = 0.014) were independent risk factors for PFS (**Table 5**). For OS, univariate analysis indicated that high SNRPD1 expression, liver capsule invasion, MVI, and vascular tumor thrombus were significantly associated ($P < 0.05$). Multivariate analysis confirmed that high SNRPD1 expression (HR = 3.16, 95% CI: 1.79-5.59, $P < 0.001$), liver capsule invasion (HR = 2.07, 95% CI: 1.22-3.53, P = 0.007), MVI (HR = 2.21, 95% CI: 1.19-4.10, P = 0.012), and vascular tumor thrombus (HR = 1.91, 95% CI: 1.11-3.27, P = 0.019) were independent risk factors for OS (**Table 6**).

Discussion

Recurrence and metastasis of HCC after liver transplantation is still the core bottleneck restricting the long-term survival of patients, and its occurrence is closely related to malignant proliferation of tumor cells, MVI, tumor angiogenesis and immune microenvironment remodeling [8, 12]. This study demonstrated for the first time that SNRPD1 was highly expressed in HCC patients after liver transplantation. Snrpd1 was an independent risk factor for progression-free survival and overall survival, and was significantly correlated with MVI, tumor MVD and immune cell infiltration pattern. SNRPD1 may participate in the progression of HCC recurrence and metastasis by simultaneously regulating tumor angiogenesis and immune microenvironment.

As a core component of the spliceosome, SNRPD1 regulates the assembly of specific spliceosomal complexes in human pluripotent stem cells. Aberrant expression of SNRPD1 can easily disrupt splicing regulation, alter the cellular transcriptome, and ultimately promote tumor initiation and progression [12, 13]. Multiple studies have confirmed that SNRPD1 is overexpressed in various cancers and is closely associated with tumor cell proliferation, invasion, and metastatic potential [9, 12-14]. Our previous study on SNRPD1 and post-hepatectomy prognosis in HCC also indicated that high SNRPD1 expression correlates with shorter OS and recurrence-free survival (RFS) [9]. In this study, SNRPD1 was further extended to the liver transplantation population to clarify the important value of SNRPD1 in the malignant progression of HCC and prognosis evaluation after transplantation.

Bioinformatics analysis revealed that SNRPD1 is significantly overexpressed in HCC tissues,

Table 2. Expression of SNRPD1 in liver cancer and adjacent tissues (n%)

Grouping	Frequency	High expression	Low expression	P
Cancer tissue	102	91	11	< 0.01
Adjacent tissue to the cancer	102	16	86	< 0.01

Table 3. Relationship between the expression level of SNRPD1 and the clinical and pathological characteristics of liver cancer patients

Grouping	Frequency (n)	High expression	Low expression	χ^2	P
Gender				0.009	0.923
Man	90	76	14		
Woman	12	10	2		
Age (years)				0.142	0.706
≤ 55	61	55	6		
> 55	41	36	5		
Number of tumors				0.631	0.427
Single	63	55	8		
Multiple	39	36	3		
Maximum diameter (cm)				0.171	0.679
≤ 5	59	52	7		
> 5	43	39	4		
Preoperative AFP (ng/ml)				1.577	0.209
≤ 400	66	57	9		
> 400	36	34	2		
Degree of differentiation				0.312	0.577
I-II	87	77	10		
III-IV	15	14	1		
Invasion of the liver capsule				1.054	0.304
No	50	43	7		
Yes	52	48	4		
MVI				8.597	5
No	34	26	8		
Yes	68	65	3		
Vascular tumor thrombus				2.995	0.083
No	49	41	8		
Yes	53	50	3		
Satellite cooker				0.051	0.822
No	77	69	8		
Yes	25	22	3		

*AFP: alpha fetoprotein, MVI: Microvascular Invasion.

Table 4. Correlation between SNRPD1 and MVD

Expression of SNRPD	High MVD	Low MVD	χ^2	r	P
High expression	65	26	6.73	0.26	< 0.01
Low expression	3	8			

*MVD: Microvascular Density.

and its differentially expressed genes are mainly enriched in viral carcinogenesis, the p53 signaling pathway, and the IL-17 signaling pathway. Dysregulation of the p53 pathway is a key factor in HCC development, while the IL-17 pathway is closely associated with the regulation of the tumor immune microenvironment [15, 16]. These findings suggest that SNRPD1 may promote HCC initiation,

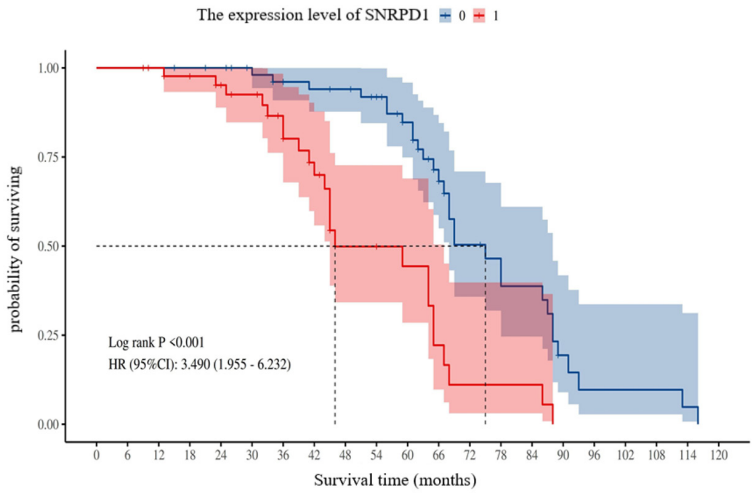

Figure 6. The PFS curve of patients with liver cancer after liver transplantation. *PFS: Progression-free Survival.

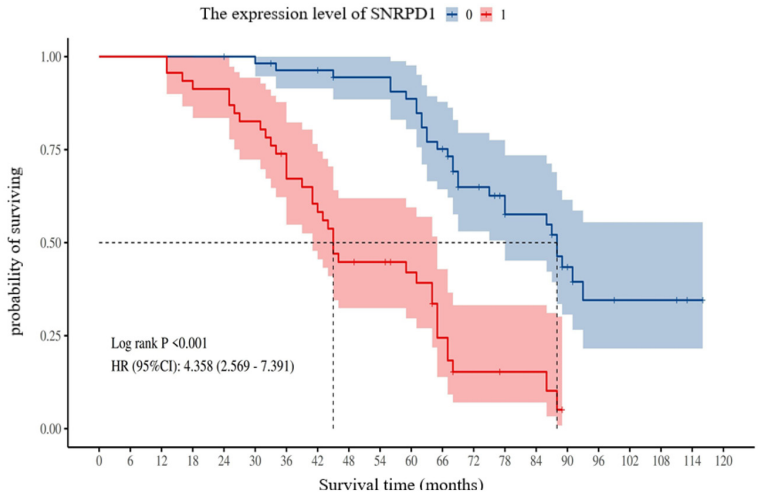

Figure 7. The OS curve of patients with liver cancer after liver transplantation. *OS: Overall Survival.

progression, and immune evasion through modulation of these pathways. Furthermore, immune cell infiltration analysis combined with Spearman correlation indicated that SNRPD1 expression in HCC tissues is significantly positively correlated with dendritic cells, B cells, CD4+ memory T cells, and CD4+ naive T cells, but negatively correlated with CD4+ central memory T cells. This suggests that SNRPD1 may participate in immune regulation by modulating the infiltration patterns of multiple immune cell types in the tumor microenvironment. Dendritic cells, as key antigen-presenting cells, play a critical role in tumor immune surveillance, and the positive correlation with SNRPD1 implies a potential regulatory role in antigen presentation, thereby affecting immune activation in HCC [17]. The positive association with B cells and CD4+ memory T cells, which are involved in initiating and maintaining tumor-specific adaptive immune responses, further indicates that SNRPD1 may positively regulate adaptive immunity in the HCC microenvironment [18]. Given that the core molecular function of SNRPD1 is the regulation of mRNA splicing, we hypothesized that SNRPD1 may regulate the alternative splicing of immune-related genes, chemokines and immune checkpoint molecules post-transcriptionally, thereby changing the chemotaxis, activation and infiltration patterns of immune cells in the tumor microenvironment. Therefore, the correlation between SNRPD1 and immune infiltration is not simply statistical correlation, but reflects its systemic influence on the immune regulatory network at the post-transcriptional level, making it a key molecule connecting HCC cell proliferation and immune regulation. The specific regulatory targets and upstream/downstream molecular mechanisms require further validation through in vitro functional assays and in vivo animal studies.

Immunohistochemical analysis in this study demonstrated that the SNRPD1 protein is specifically localized to the nuclei of HCC cells, with a significantly higher positive expression rate in tumor tissues compared to adjacent non-tumor tissues, suggesting its role as a nuclear functional protein in hepatocarcinogenesis. Clinicopathological analysis revealed that SNRPD1 expression was significantly associated only with MVI, and showed no correlation with patient sex, age, tumor size or number, histological differentiation, AFP levels, liver capsule

Table 5. Univariate and multivariate COX analyses of factors affecting PFS

Clinical data	Univariate analysis		Multivariate analysis	
	HR (95% CI)	P	HR (95% CI)	P
The expression of SNRPD1	3.49 (1.95-6.23)		2.08 (1.09-3.95)	0.025
Gender	1.10 (0.46-2.62)	0.835	-	-
Age	1.33 (0.76-2.32)	0.315	-	-
Number of tumors	1.28 (0.74-2.21)	0.376	-	-
Maximum diameter	1.39 (0.80-2.42)	0.246	-	-
Preoperative AFP	1.10 (0.60-2.01)	0.756	-	-
Tumor differentiation	0.43 (0.16-1.14)	0.088	-	-
Hepatic capsule invasion	3.43 (1.85-6.38)	1	3.25 (1.51-6.98)	0.003
MVI	1.85 (0.92-3.73)	0.084	2.10 (1.12-3.92)	0.020
Vascular tumor thrombus	2.53 (1.39-4.61)	0.002	2.34 (1.19-4.64)	0.014
Satellite lesion	2.32 (1.24-4.34)	0.008	0.86 (0.40-1.85)	0.708

*PFS: Progression-free Survival, HR: Hazard Ratio, CI: Confidence Interval, AFP: Alpha Fetoprotein, MVI: Microvascular Invasion.

Table 6. Univariate and multivariate COX analyses of factors affecting OS

Clinical data	Univariate analysis		Multivariate analysis	
	HR (95% CI)	P	HR (95% CI)	P
The expression of SNRPD1	4.36 (2.57-7.39)	< 0.001	3.16 (1.79-5.59)	< 0.001
Gender	1.12 (0.51-2.45)	0.785	-	-
Age	1.35 (0.82-2.22)	0.236	-	-
Number of tumors	1.11 (0.67-1.85)	0.690	-	-
Maximum diameter	1.25 (0.76-2.04)	0.378	-	-
Preoperative AFP	1.53 (0.93-2.53)	0.094	-	-
Tumor differentiation	0.96 (0.46-2.02)	0.917	-	-
Hepatic capsule invasion	2.27 (1.36-3.79)	0.002	2.07 (1.22-3.53)	0.007
MVI	2.53 (1.40-4.58)	0.002	2.21 (1.19-4.10)	0.012
Vascular tumor thrombus	2.58 (1.53-4.35)	1	1.91 (1.11-3.27)	0.019
Satellite lesion	1.61 (0.91-2.86)	0.105	-	-

*OS: Overall Survival, HR: Hazard Ratio, CI: Confidence Interval, AFP: Alpha Fetoprotein, MVI: Microvascular Invasion.

invasion, vascular tumor thrombi, or satellite lesions. Given that MVI is a key risk factor for post-liver transplantation recurrence in HCC, these findings indicate that SNRPD1 may serve as a potential molecular marker for predicting recurrence risk after transplantation [9]. Spearman correlation analysis further showed a significant positive association between SNRPD1 expression and MVD in HCC tissues, suggesting that SNRPD1 may promote MVI formation through regulation of tumor angiogenesis, thereby increasing the risk of post-transplant recurrence.

Survival analysis revealed that patients with high SNRPD1 expression had significantly shorter median PFS and OS compared to those with low expression (both $P < 0.001$), indicating that elevated SNRPD1 is closely associated with increased post-liver transplantation recurrence risk and poorer prognosis. Univariate Cox regression confirmed the prognostic value of traditional indicators such as liver capsule invasion, MVI, and vascular tumor thrombi for PFS and OS after HCC transplantation, consistent with previous studies, and, for the first time, demonstrated a significant association between high SNRPD1 expression and postoperative PFS and OS in this population [19-21]. Multivariate analysis further verified that high SNRPD1 expression is an independent risk factor for PFS (HR = 2.08, 95% CI: 1.09-3.95, $P = 0.025$) and OS (HR = 3.16, 95% CI: 1.79-5.59, $P < 0.001$). Additionally, liver capsule invasion and vascular tumor thrombi were independent risk factors for PFS, while liver capsule inva-

sion, MVI, and vascular tumor thrombi were independent risk factors for OS. These findings suggest that SNRPD1 could serve as a novel and meaningful biomarker for assessing recurrence and survival risk in HCC patients following liver transplantation.

Moreover, this study only included HCC patients who met the Hangzhou criteria for liver transplantation, a rigorously selected subgroup with relatively favorable prognoses. Therefore, our findings regarding SNRPD1 as a prognostic marker may not be directly generalizable to all HCC patients, particularly those with advanced stage or who are beyond transplantation criteria. Future studies should validate the role of SNRPD1 in broader HCC cohorts, including patients receiving resection, ablation, or systemic therapies.

This study is the first to investigate the role of SNRPD1 in prognostic assessment within the context of liver transplantation for HCC. SNRPD1 may be combined with traditional pathological indicators to construct more precise postoperative prognostic models, providing a valuable reference for individualized clinical follow-up and intervention. Since this is a single-center retrospective study with a limited sample size, the conclusions obtained are preliminary and based only on liver transplant recipients screened according to the Hangzhou criteria, and therefore cannot be extrapolated to all patients with hepatocellular carcinoma. In the future, multi-center studies and basic experiments are needed to verify the results and the underlying mechanism.

Acknowledgements

This work was supported by the Fujian Natural Science Foundation (2023J011348).

Disclosure of conflict of interest

None.

Address correspondence to: Fang Yang, Department of Hepatobiliary Surgery, 900th Hospital of PLA Joint Logistic Support Force, No. 156 The Second West Ring Road, Fuzhou 350025, Fujian, China. Tel: +86-13960821932; E-mail: Yfang105@163.com

References

[1] Bray F, Laversanne M, Sung H, Ferlay J, Siegel RL, Soerjomataram I and Jemal A. Global cancer statistics 2022: GLOBOCAN estimates of incidence and mortality worldwide for 36 cancers in 185 countries. CA Cancer J Clin 2024; 74: 229-263.

[2] Zhang Y, Wang Y, Guo JH and Lu J. Current trends in hepatocellular carcinoma therapies in China. Dig Dis Interv 2024; 8: 173-182.

[3] Llovet JM, Kelley RK, Villanueva A, Singal AG, Pikarsky E, Roayaie S, Lencioni R, Koike K, Zucman-Rossi J and Finn RS. Hepatocellular carcinoma. Nat Rev Dis Primers 2021; 7: 6.

[4] Siegel RL, Miller KD, Fuchs HE and Jemal A. Cancer statistics, 2021. CA Cancer J Clin 2021; 71: 7-33.

[5] Adams R, Brown K, Zhang Y, et al. Liver transplantation for HCC. J Hepatol 2019; 71: 678-689.

[6] Ma S, Li X, Wang X, Cheng L, Li Z, Zhang C, Ye Z and Qian Q. Current progress in CAR-T cell therapy for solid tumors. Int J Biol Sci 2019; 15: 2548-2560.

[7] Leung AK, Nagai K and Li J. Structure of the spliceosomal U4 snRNP core domain and its implication for snRNP biogenesis. Nature 2011; 473: 536-539.

[8] Wang H, Chen M, Yang C, Hu H, Jiang Y, Yang F and Lv L. SNRPD1 inhibition suppresses the proliferation of hepatocellular carcinoma and promotes autophagy through the PI3K/AKT/mTOR/4EBP1 pathway. Arch Biochem Biophys 2023; 743: 109661.

[9] Wang H, Xu F, Lu L, Yang F, Huang X, Lv L, Hu H and Jiang Y. The diagnostic and prognostic significance of small nuclear ribonucleoprotein Sm D1 aberrantly high expression in hepatocellular carcinoma. J Cancer 2022; 13: 184-201.

[10] Batra R, Harder N, Gogolin S, Diessl N, Soons Z, Jäger-Schmidt C, Lawerenz C, Eils R, Rohr K, Westermann F and König R. Time-lapse imaging of neuroblastoma cells to determine cell fate upon gene knockdown. PLoS One 2012; 7: e50988.

[11] Dai X, Cai L, Zhang Z and Li J. SNRPD1 conveys prognostic value on breast cancer survival and is required for anthracycline sensitivity. BMC Cancer 2023; 23: 376.

[12] Liu G, Li F, Chen M, Luo Y, Dai Y and Hou P. SNRPD1/E/F/G serve as potential prognostic biomarkers in lung adenocarcinoma. Front Genet 2022; 13: 813285.

[13] Dai X, Yu L, Chen X and Zhang J. SNRPD1 confers diagnostic and therapeutic values on breast cancers through cell cycle regulation. Cancer Cell Int 2021; 21: 229.

[14] Quidville V, Alsafadi S, Goubar A, Commo F, Scott V, Pioche-Durieu C, Girault I, Baconnais S, Le Cam E, Lazar V, Delaloge S, Saghatchian M, Pautier P, Morice P, Dessen P, Vagner S and André F. Targeting the deregulated spliceosome core machinery in cancer cells triggers mTOR blockade and autophagy. Cancer Res 2013; 73: 2247-2258.
[15] Tan Y, Zhou Y, Zhang W, Wu Z, Xu Q, Wu Q, Yang J, Lv T, Yan L, Luo H, Shi Y and Yang J. Repaglinide restrains HCC development and progression by targeting FOXO3/lumican/p53 axis. Cell Oncol (Dordr) 2024; 47: 1167-1181.
[16] Gorczynski RM. IL-17 signaling in the tumor microenvironment. Adv Exp Med Biol 2020; 1240: 47-58.
[17] Steinman RM and Banchereau J. Taking dendritic cells into medicine. Nature 2007; 449: 419-426.
[18] Coussens LM and Werb Z. Inflammation and cancer. Nature 2002; 420: 860-867.
[19] Zeng Q, Lei F, Chang Y, Gao Z, Wang Y, Gao Q, Niu P and Li Q. An oncogenic gene, SNRPA1, regulates PIK3R1, VEGFC, MKI67, CDK1 and other genes in colorectal cancer. Biomed Pharmacother 2019; 117: 109076.
[20] Tabrizian P, Jibara G, Shrager B, Schwartz M and Roayaie S. Recurrence of hepatocellular cancer after resection: patterns, treatments, and prognosis. Ann Surg 2015; 261: 947-955.
[21] Kılcı BM, İnce V, Carr BI, Usta S, Bağ HG, Şamdancı E, Işık B and Yılmaz S. Parameters predicting microvascular invasion and poor differentiation in hepatocellular carcinoma patients with normal alpha-fetoprotein level before liver transplantation. Turk J Gastroenterol 2023; 34: 753-759.